Supporting Information

Ultrahigh-rate nickel monosulfide anodes for sodium/potassium-ion storage

Milan K. Sadan[a], Huihun Kim[a], Changhyeon Kim[a], Gyu-Bong Cho[b], Kwon-Koo Cho[b], Jou-Hyeon Ahn[b]*, and Hyo-Jun Ahn[b]*

[a]*Research Institute for Green Energy Convergence Technology, Gyeongsang National University, Jinju 52828, Republic of Korea*

[b]*Department of Materials Engineering and Convergence Technology*, RIGET, Gyeongsang National University, Jinju 52828, Republic of Korea

*Corresponding authors
E-mail addresses: ahj@gnu.ac.kr (HJA) and jhahn@gnu.ac.kr (JHA)

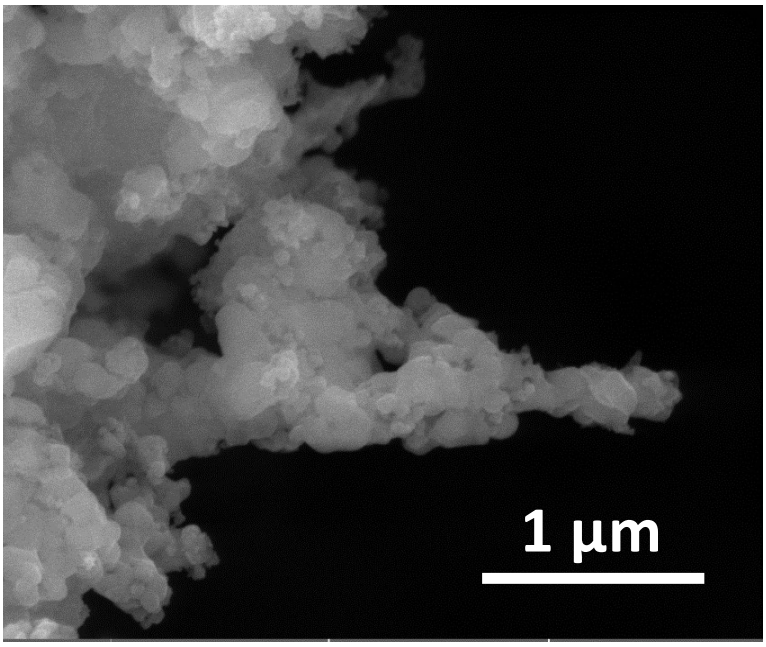

Fig. S1 Field-emission scanning electron microscopy (FESEM) image of nickel monosulfide (NiS) nanoparticles.

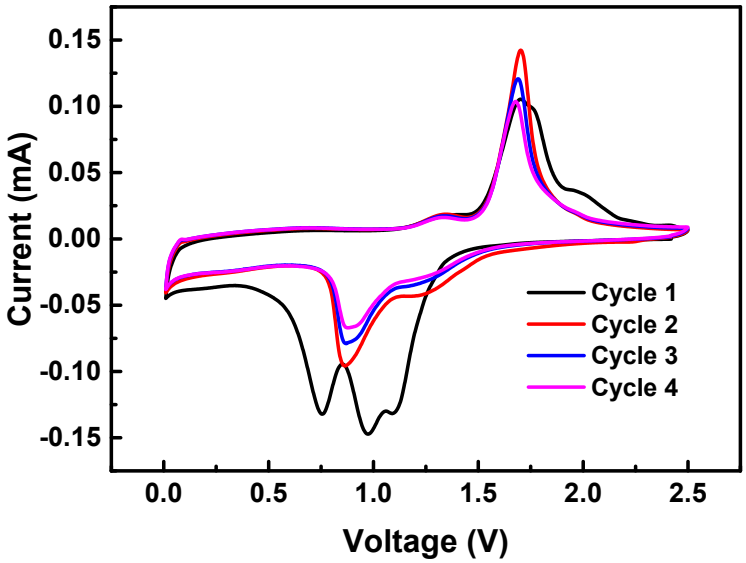

Fig. S2 Cyclic voltammograms of the NiS electrode in a carbonate electrolyte at a scan rate of 0.1 mV s^{-1} for sodium ion batteries.

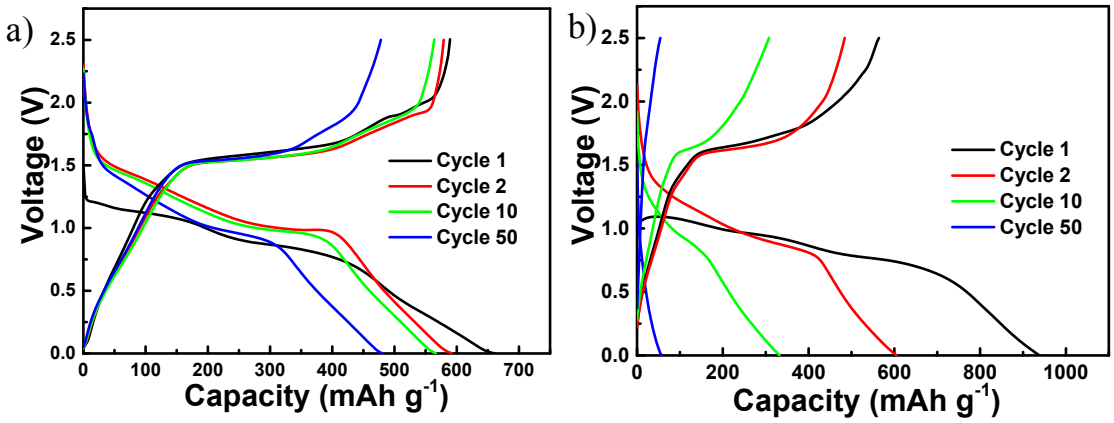

Fig. S3 Voltage profiles of the NiS electrode recorded in a) ether and b) carbonate electrolytes at a current density of 1 A g^{-1} for sodium ion batteries.

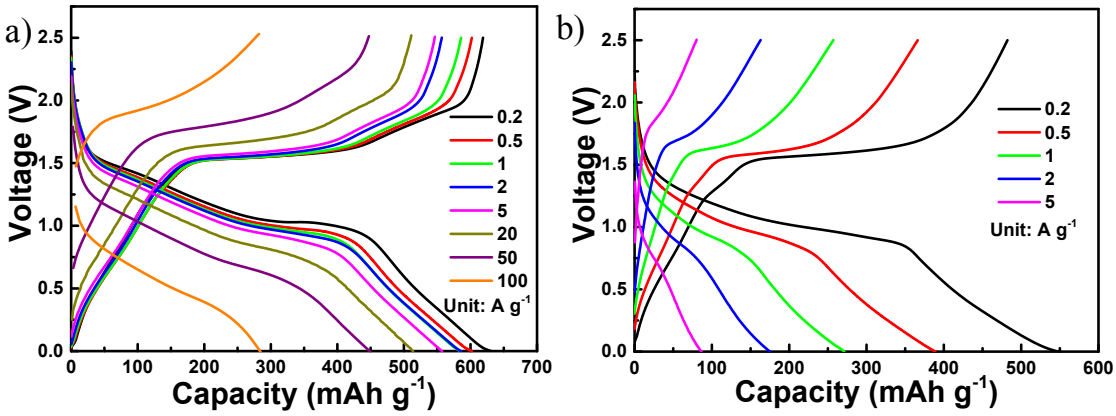

Fig. S4 Voltage profiles reflecting the rate performances of the NiS electrode in a) ether and b) carbonate electrolytes for sodium ion batteries.

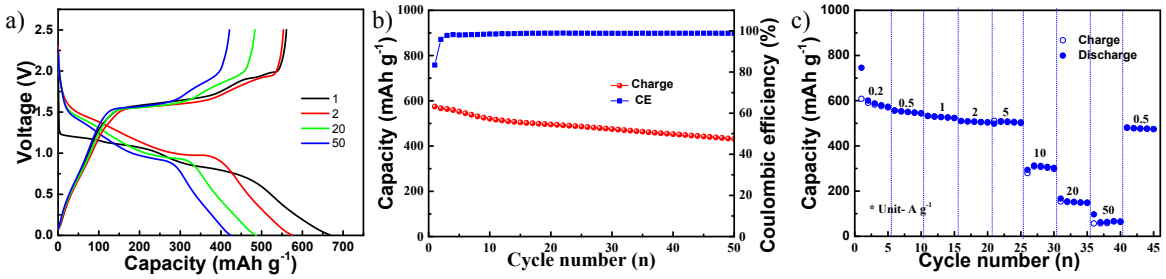

Fig. S5 a) Voltage profiles and b) corresponding cycling performance and c) rate performance of the NiS electrode with high loading (2.54 g/cm^2) in sodium ion batteries.

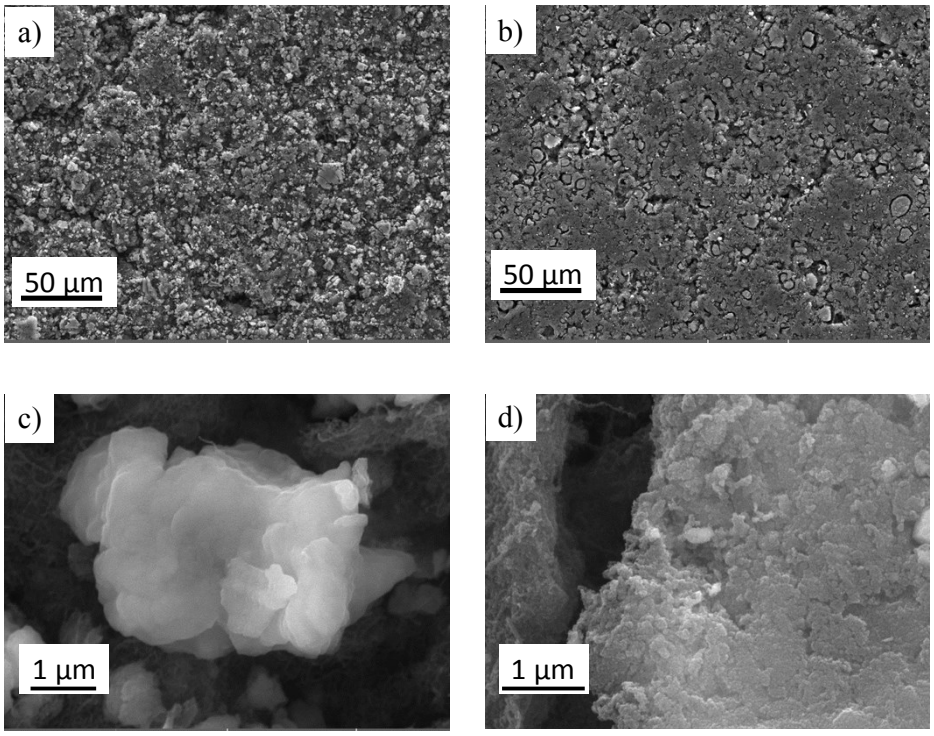

Fig. S6 FESEM images of the NiS electrode obtained after cycling in a,c) carbonate and b,d) ether electrolytes for sodium ion batteries.

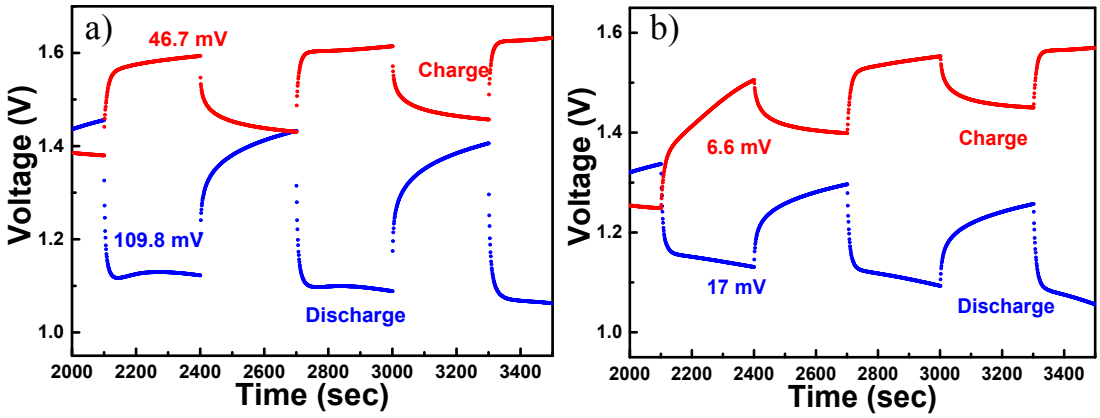

Fig. S7 Galvanostatic intermittent titration technique (GITT) profiles of the NiS electrode recorded in a) carbonate and b) ether electrolytes for sodium ion batteries.

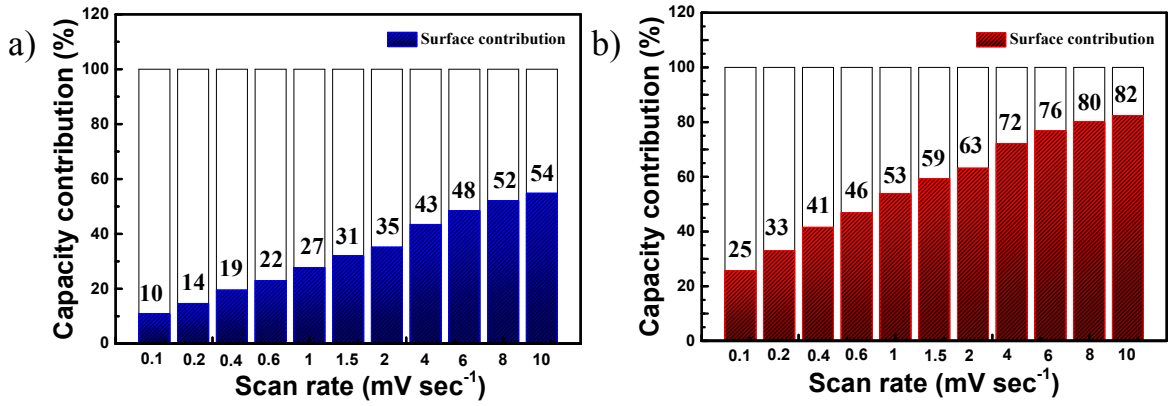

Fig. S8 The contribution ratio of diffusion-controlled and surface-controlled behavior at different scan rates in both a) carbonate and b) ether electrolytes for sodium ion batteries.

Table S1 Comparison of the results obtained in this work with those of the previous studies on NiS

Sl. No.	Electrode	Electrolyte	Carbon Content (%)	Current collector	First reversible capacity (mAh g^{-1})	Initial coulombic efficiency (%)	Rate performance (mAh g^{-1})	Ref
1	NiS plates	1 M $NaClO_4$ in PC + 5 % FEC	38	Cu	381 (1A g^{-1})	49	43 (10 A g^{-1})	S1
2	NiS spheres	1 M $NaClO_4$ in PC + 5 % FEC	Not mentioned	Cu	683 (0.1 A g^{-1})	73	337 (5 A g^{-1})	S2
3	CNT@NiS/C	1 M $NaClO_4$ in EC/DEC	35	Cu	418 (0.1 A g^{-1})	60	–	S3
4	NiS/2D nanosheet	1 M $NaClO_4$ in EC/PC + 5 % FEC	36	Cu	544 (0.2 A g^{-1})	77.2	393 (2 A g^{-1})	S4
5	Hollow NiS @CNF	1 M $NaCF_3SO_3$ in EC/DEC	25.1	Cu	324.4 (1 A g^{-1})	71.2	274.7 (5 A g^{-1})	S5
6	acicular NiS-Ni	1 M $NaPF_6$ in EC/DEC/DMC+ 5% FEC	–	Ni	813.6 (0.1 A g^{-1})	59.2	332.3 (0.4 A g^{-1})	S6
7	NiS/MoS_2/C	1 M $NaClO_4$ in EC/DMC + 5% FEC	7.4	Cu	571 (0.1 A g^{-1})	80.2	398 (5 A g^{-1})	S7
8	NiS/C flower	1 M $NaClO_4$ in DEGDME	Not mentioned	Cu	776 (0.1 A g^{-1})	74	110 (3 A g^{-1})	S8
9	NiS nanoneedles	1 M $NaPF_6$ in DME	3	Cu	597 (0.1 A g^{-1})	93	320 (20 A g^{-1})	S9
10	NiS@N doped C	1 M $NaClO_4$ in EC/DEC + 5% FEC	17.2	Not mentioned	824 (0.1 A g^{-1})	–	688(3.2 A g^{-1})	S10

11	NiS nanoparticle	1 M $NaPF_6$ in DME	–	Carbon coated Aluminum	589 (1A g^{-1})	89	286 (100 A g^{-1})	This report

$NaClO_4$: Sodium perchlorate, $NaCF_3SO_3$: Sodium trifluoromethanesulfonate, $NaPF_6$: Sodium hexafluorophosphate, PC: Propylene carbonate, EC: Ethylene carbonate, FEC: Fluoroethylene carbonate, DEC: Diethyl carbonate, DMC: Dimethyl carbonate, DEGDME: diglycol methyl ether, DME: dimethyl ether.

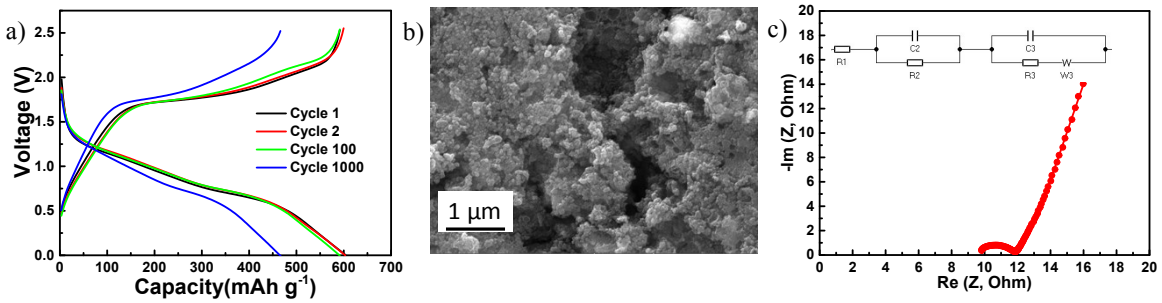

Fig. S9 a) Voltage profiles recorded during cycling at a current density of 25 A g^{-1}. b) FESEM image and c) Nyquist plot of the NiS electrode after 1000 cycles for sodium ion batteries.

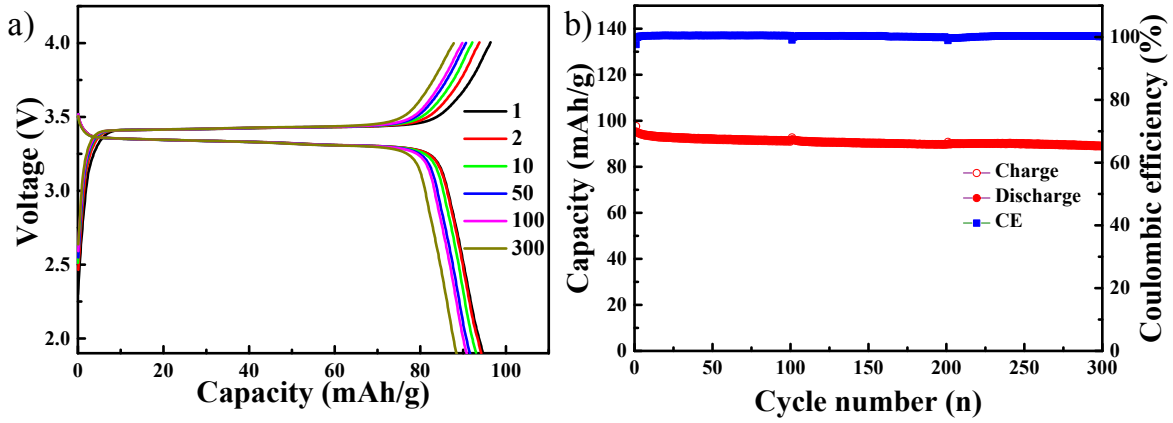

Fig. S10 a) Voltage profile and corresponding cycling performance of NVP cathode at current density of 1.17 A g^{-1}.

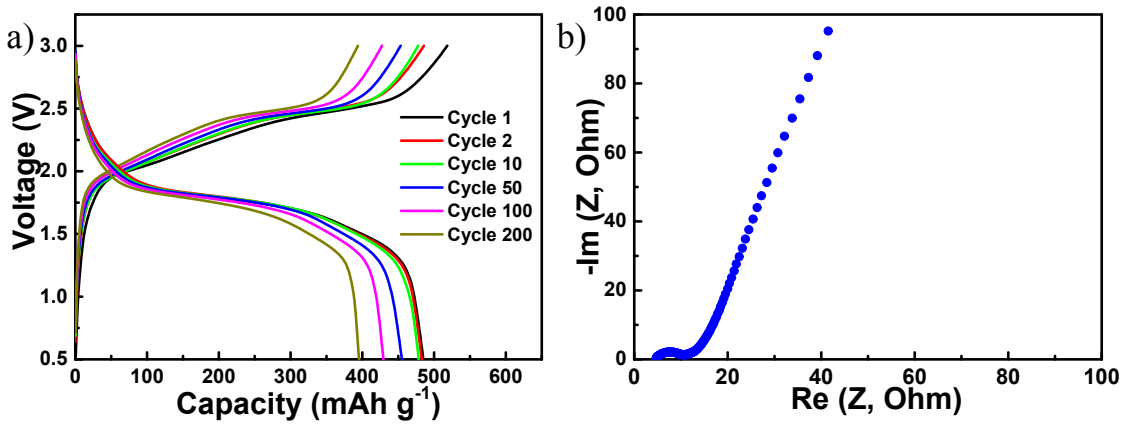

Fig. S11 a) Voltage profiles recorded during cycling at 2 A g^{-1}. b) Electrochemical impedance spectrum obtained after cycling the $Na_3V_2(PO_4)$ (NVP)/NiS full-cell.

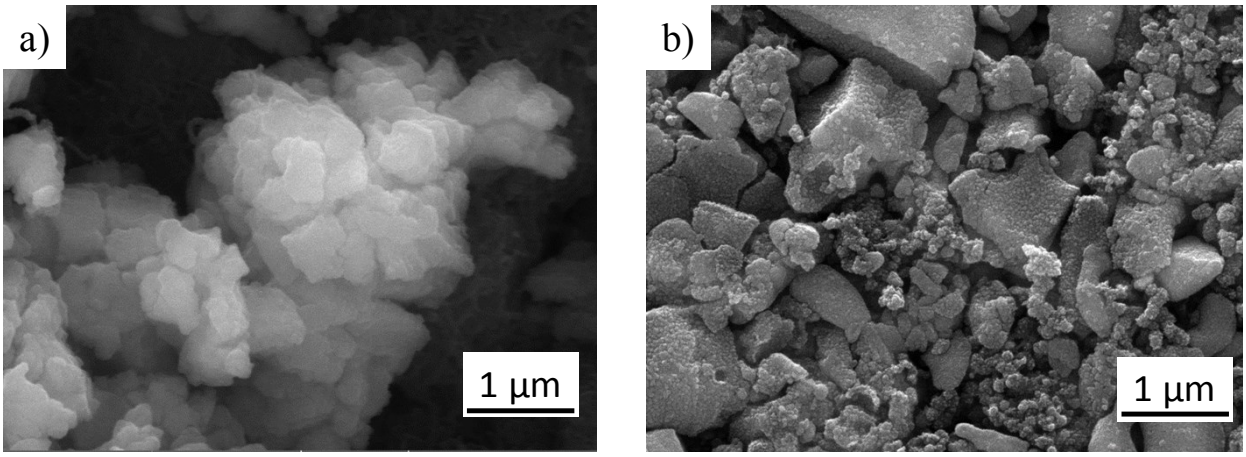

Fig. S12 FESEM images of the a) NiS anode and b) NVP cathode after cycling.

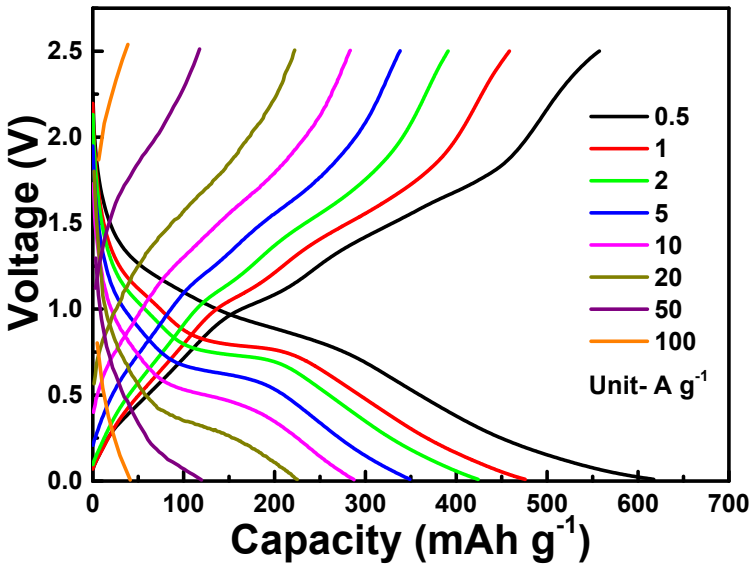

Fig. S13 Voltage profiles presenting the rate performance of the NiS electrode in a potassium-ion battery.

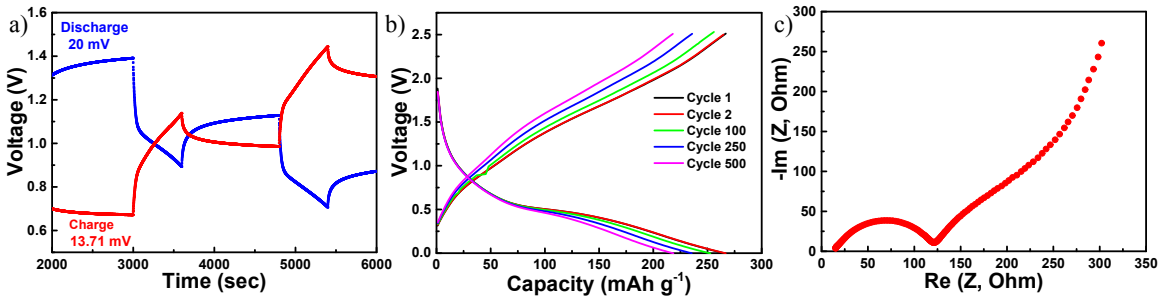

Fig. S14 a) GITT profiles, b) voltage profiles recorded during cycling at a current rate of 10 A g^{-1}, and c) Nyquist plot obtained after the long-term cycling of the NiS electrode in a potassium-ion battery.

References

S1. H. Fan, H. Yu, X. Wu, Y. Zhang, Z. Luo, H. Wang, Y. Guo, S. Madhavi and Q. Yan, *ACS Appl Mater Interfaces.*, 2016, **8**, 25261-25267. https://doi.org/10.1021/acsami.6b07300.

S2. D. Zhang, W. Sun, Y. Zhang, Y. Dou, Y. Jiang and S. X. Dou, *Adv. Funct. Mater.,* 2016, **26**, 7479-7485, https://doi.org/10.1002/adfm.201602933.

S3. F. Han, C. Y. J. Tan and Z. Gao, *Energy Technol.,* 2017, **5**, 580-587, https://doi.org/10.1002/ente.201600393.

S4. J. Wang, D. Cao, G. Yang, Y. Yang and H. Wang, *J Solid State Electrochem.*, 2017, **21**, 3047-3055, https://doi.org/10.1007/s10008-017-3600-9.

S5. Y. Zhang, C. Lv, X. Wang, S. Chen, D. Li, Z. Peng and D. Yang, *ACS Appl Mater Interfaces.*, 2018, **10**, 40531-40539, https://doi.org/10.1021/acsami.8b13805.

S6. Q. Chen, S. Ni, J. Tang, T. Li, T. Kang and X. Yang, *Mater. Lett.,* 2018, **213**, 193-196, https://doi.org/10.1016/j.matlet.2017.11.061.

S7. H. Xie, M. Chen and L. Wu, *ACS Appl Mater Interfaces.*, 2019, **11**, 41222-41228, https://doi.org/10.1021/acsami.9b11078.

S8. G. Xia, X. Li, Y. Gu, P. Dong, Y. Zhang, J. Duan, D. Wang and Y. Zhang, *Ionics.*, 2020, **27**, 191-197, https://doi.org/10.1007/s11581-020-03818-9.

S9. T. Li, H. Li, A. Qin, H. Wu, D. Zhang and F. Xu, *J. Power Sources,* 2020, **451**, 227796, https://doi.org/10.1016/j.jpowsour.2020.227796.

S10. X. Zhao, F. Gong, Y. Zhao, B. Huang, D. Qian, H.-E. Wang, W. Zhang and Z. Yang, *Chem. Eng. J.,* 2020, **392**, https://doi.org/10.1016/j.cej.2019.123675.